J Gastroenterol (2014) 49:263–269
DOI 10.1007/s00535-013-0887-x

The Japanese Society of Gastroenterology

ORIGINAL ARTICLE—ALIMENTARY TRACT

Modeling of stem cell dynamics in human colonic crypts in silico

Yuki Kagawa · Noriko Horita · Hideki Taniguchi · Satoshi Tsuneda

Received: 29 May 2013 / Accepted: 12 September 2013 / Published online: 30 September 2013

Abstract
Background Several possible scenarios of cellular dynamics in human colonic crypts have been inferred from transgenic animal experiments. However, because of the discrepancy in size and physiology between humans and animals, quantitative predictions of tissue renewal and cancer development are difficult to execute.
Methods A two-dimensional individual based model was developed for the first time to predict cellular dynamics in human colonic crypts. A simple scenario, in which stem cells were not fixed positionally, divide symmetrically and asymmetrically in a stochastic fashion in the lower part of the crypt, was proposed and implemented in the developed model. Numerical simulations of the model were executed in silico.
Results By comparing the results of computational simulations with available experimental data, the presented scenario was consistent with various experimental evidence. Using this scenario, we simulated and visualized monoclonal conversion in the human colonic crypt. We also predicted that the propensity for monoclonal expansion of a mutant cell was largely dependent on the phenotype, the cell type, the position and the state of the crypt.
Conclusions Using the computational framework developed in this study, model users can verify possible scenarios of stem cell dynamics occurring in human colonic crypts and quantitatively predict cell behavior. Its applicability in scenario verification and predictability makes it a valuable tool for elucidation of stem cell dynamics in human colonic crypts.

Keywords Individual based model · Mathematical modeling · Monoclonal conversion · Mutation accumulation

Introduction

In recent studies using transgenic mice, several hypotheses of tissue renewal and cancer development occurring in intestinal epithelia have been directly tested by expressing specific genes in specific cell types. For example, Barker et al. [1] showed that specific deletion of the adenomatous polyposis coli gene in leucine-rich repeat G protein-coupled receptor 5 (Lgr5)-expressing cells results in development of macroscopic adenomas within 3–5 weeks. Tian et al. [2] specifically expressed the human diphtheria toxin receptor gene in Lgr5-expressing cells to ablate this cell type by diphtheria toxin administration, and revealed the dispensability of Lgr5-expressing cells for normal intestinal homeostasis.

Such direct verifications of hypotheses are usually difficult in humans. Instead of specifically expressing reporter

Electronic supplementary material The online version of this article (doi:10.1007/s00535-013-0887-x) contains supplementary material, which is available to authorized users.

Y. Kagawa
Institute for Nanoscience and Nanotechnology, Waseda University, 2-2 Wakamatsu-cho, Shinjuku-ku, Tokyo 162-8480, Japan

N. Horita · S. Tsuneda (✉)
Department of Life Science and Medical Bioscience, Waseda University, 2-2 Wakamatsu-cho, Shinjuku-ku, Tokyo 162-8480, Japan
e-mail: stsuneda@waseda.jp

H. Taniguchi
Department of Regenerative Medicine, Yokohama City University Graduate School of Medicine, 3-9 Fukuura, Kanazawa-ku, Yokohama 236-0004, Japan

genes in stem cells, tracks of cell lineages in human intestinal tissues were experimentally imaged by staining cytochrome c oxidase (CCO)-deficient (CCO–) cells [3]. CCO is a mitochondrially encoded enzyme that shows sporadic loss of expression with aging. Imaging of CCO– cells revealed that a CCO– stem cell can occupy the whole crypt via niche succession, which leads to monoclonal conversion of the whole crypt. Another strategy evaluates the methylation patterns of non-expressed genes to determine the rates of recent clonal expansion of stem cells [4, 5]. However, methylation patterns dynamically change with time [6]. In addition, demethylation and methylation rates appear to be significantly different between genetic loci. This observation suggests that the results derived from methylation analyses are strongly influenced by the choice of CpG islands to analyze. Therefore, methylation markers are poorly suited to conclude the cell lineage status and clonality of cell populations in intestinal crypts [7]. Because of these difficulties, the dynamics of tissue renewal in the human intestinal tract is usually inferred from experimental results using transgenic mice. However, the intestinal tracts of mice and humans are different in size (250 vs. 2,000 cells in each intestinal crypt) and physiology (2–3 vs. 3–5 days for tissue renewal). Thus, quantitative predictions of cell behavior in the human intestinal tract are difficult.

To complement experimental approaches, theoretical approaches have been proposed. For example, Johnston et al. [8] developed models to describe the dynamics in populations of stem, transit amplifying (TA), and differentiated cells in the crypt without spatial information. To quantitatively compare simulation results with spatial experimental data, Boman et al. [9] developed models that describe cell population dynamics at each cell position in a crypt. However, to describe the spatial distribution of each cell type in a crypt, individual-based (IB) models that treat each cell as an individual are appropriate. Two- and three-dimensional IB models, including several of signaling dynamics, have been developed to describe tissue renewal in mouse intestinal crypts [10–12]. In the present study, we describe an IB modeling framework for a human intestinal crypt. One of the strengths of this computational framework is its ability to implement various possible scenarios of stem cell dynamics and to visualize their cell population dynamics in a human colonic crypt in silico.

Methods

Model development

The outline of the human colonic crypt model is shown in Fig. 1a. Human colonic crypts with a height of 82 cells were modeled as a cylinder, in which cells proliferated and differentiated independently. Three cell types were considered, namely stem, TA and differentiated cells. Each cell was modeled as a circle with an increasing radius as time progressed to represent growth. When the cell radius reached the critical value, the cell divided into two new cells. For each time step, the spatial arrangement of cells in the crypt was calculated by shoving cells when they became too close to each other. To implement this process, rather than solving the equations of motion, we used a 'shoving' algorithm that was originally developed for the multi-species biofilm model [13]. Using this algorithm, we substantially reduced the calculation load. Rules of cell division and differentiation were determined by the scenario defined by the model user. Here, we used the scenario defined in Fig. 1b. Details of the model including the proposed scenario and the algorithm used were presented in the supplementary text A provided as Electronic Supplementary Material.

Numerical simulations

After implementing a scenario to the developed model, numerical simulations of the model were executed as follows. First, an assigned number of stem cells was arranged at the bottom of the crypt. Then, using the shoving algorithm, cells shoved each other to minimize the overlapping area. As time progressed, cell division occurred, which was ruled by each scenario. After several rounds of the cell cycle, cells belonging to all of the three cell types occupied the crypt. Any cell with a center that exceeded the top of the crypt was deleted. Cell number reached a steady state at about 15 days from the start.

Results

Cell dynamics in human colonic crypts in a steady state

Figure 1c shows a snapshot of the crypt in a steady state (also see Video 1 provided as Electronic Supplementary Material). The four model parameter values were determined to be consistent with the quantitative data, i.e. the probability of finding labeled cells at a given cell position, obtained in bromodeoxyuridine (BrdU) pulse labeling experiments using a large number of human colonic crypts (see Fig. 1d, e) [14]. The details of the calibration of the model parameters are described in the supplementary text B provided as Electronic Supplementary Material.

As shown in Video 1, some differentiated cells positioned near the stem cells appeared to remain in the crypt for a relatively long period of time. We have discussed this observation in the supplementary text A.

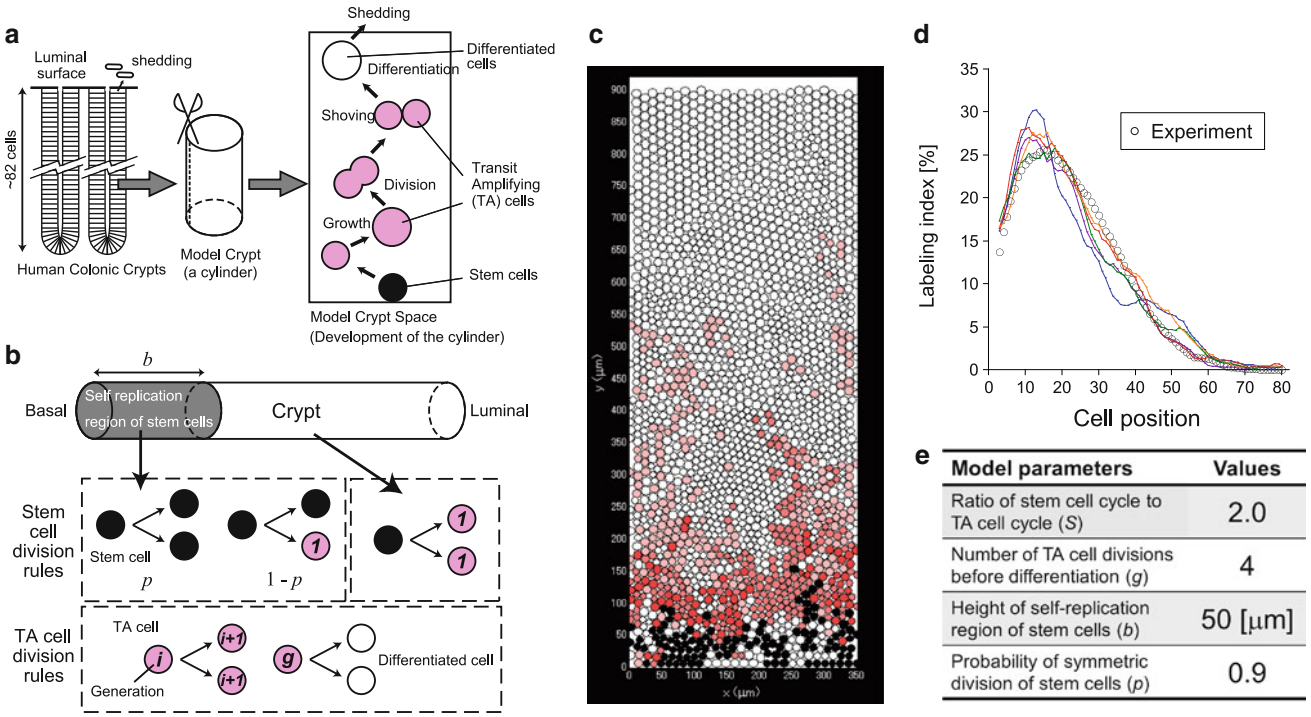

Model parameters	Values
Ratio of stem cell cycle to TA cell cycle (*S*)	2.0
Number of TA cell divisions before differentiation (*g*)	4
Height of self-replication region of stem cells (*b*)	50 [μm]
Probability of symmetric division of stem cells (*p*)	0.9

Fig. 1 **a** Outline of the human colonic crypt model. The crypt is modeled as a cylinder. Cells in the crypt grow, proliferate, shove and differentiate on the developed surface of the cylinder. Cells are shed from the surface at the upper end. We considered three cell types: stem (*black*), transit amplifying (TA; *pink*) and differentiated cells (*white*). **b** The simulated scenario of cell proliferation and differentiation. We defined the self-replication region of stem cells as the lower b μm part of the crypt. Within this region, a stem cell divides symmetrically and produces two stem cells with a probability p ($0 \leq p \leq 1$), or divides asymmetrically and produces a stem cell and a TA cell with a probability $1 - p$. On the outside, stem cells divide symmetrically and produce two first-generation TA cells. Regardless of the region, TA cells divide symmetrically and differentiate after g divisions. Index i on each TA cell represent its generation. **c** Snapshots of the model crypt in a steady state. *Black*, *red*, and *white* represent stem, TA, and differentiated cells, respectively. *Dark red* represents low generation of TA cells. **d** Fitting to BrdU labeling experimental data obtained from human colonic crypts. Experimental data: *open circles*. Simulation data: *curves*. *Curve color* represents individual simulations using the same parameter sets. **e** Model parameter values used in the simulation. See the supplementary text A provided in Electronic Supplementary Material for details

Clonal expansion dynamics

Clonal expansion and conversion to monoclonality has been observed experimentally in mouse colonic crypts [15]. Experimental evidences [3, 6, 16] strongly imply that the same monoclonal conversions occur in human colonic crypts. In the constructed model, monoclonal conversions occurred as shown in Fig. 2a (also see Video 2 provided as Electronic Supplementary Material). In such a case, cells were stained with various colors at an arbitrary time point ($t = 0$). Then, the descendants of these cells with their color the same as the mothers' formed clonal cell groups. The number of groups decreased with time, and ultimately, monoclonal conversion in the crypt occurred at $t = 1{,}300$ h. Figure 2b shows the corresponding spatial distribution of cell types for each image shown in Fig. 2a. By comparing these figures, a single stem cell positioned at the bottom of the crypt at time $t = 0$ produced all cells including stem, TA, and differentiated cells at $t = 1{,}300$ h. Cell position in a crypt was a critical factor for monoclonal expansion of the cell in the crypt. In fact, cells that were not positioned at the bottom of the crypt were washed out from the crypt as time progressed, and monoclonal expansion of such cells did not occur.

Monoclonal expansion of a mutant cell

Colon cancer occurs as a consequence of the accumulation of several somatic mutations in a crypt through evolutional dynamics [17–21]. To accumulate mutations, mutant cells must remain in the crypt. This phenomenon may occur as a result of clonal expansion of mutated cells in the crypt. Regarding the evolution dynamics of cancer, whether the propensity for mutation accumulation changes with the phenotype of the mutation is particularly interesting. Using the proposed model, whether a single mutant cell occupied the whole crypt was simulated, and the probability of occurrence of monoclonal expansion of the mutant cell (P_{accum}) was calculated. The mutation was represented by a set of parameter values that characterized the mutant

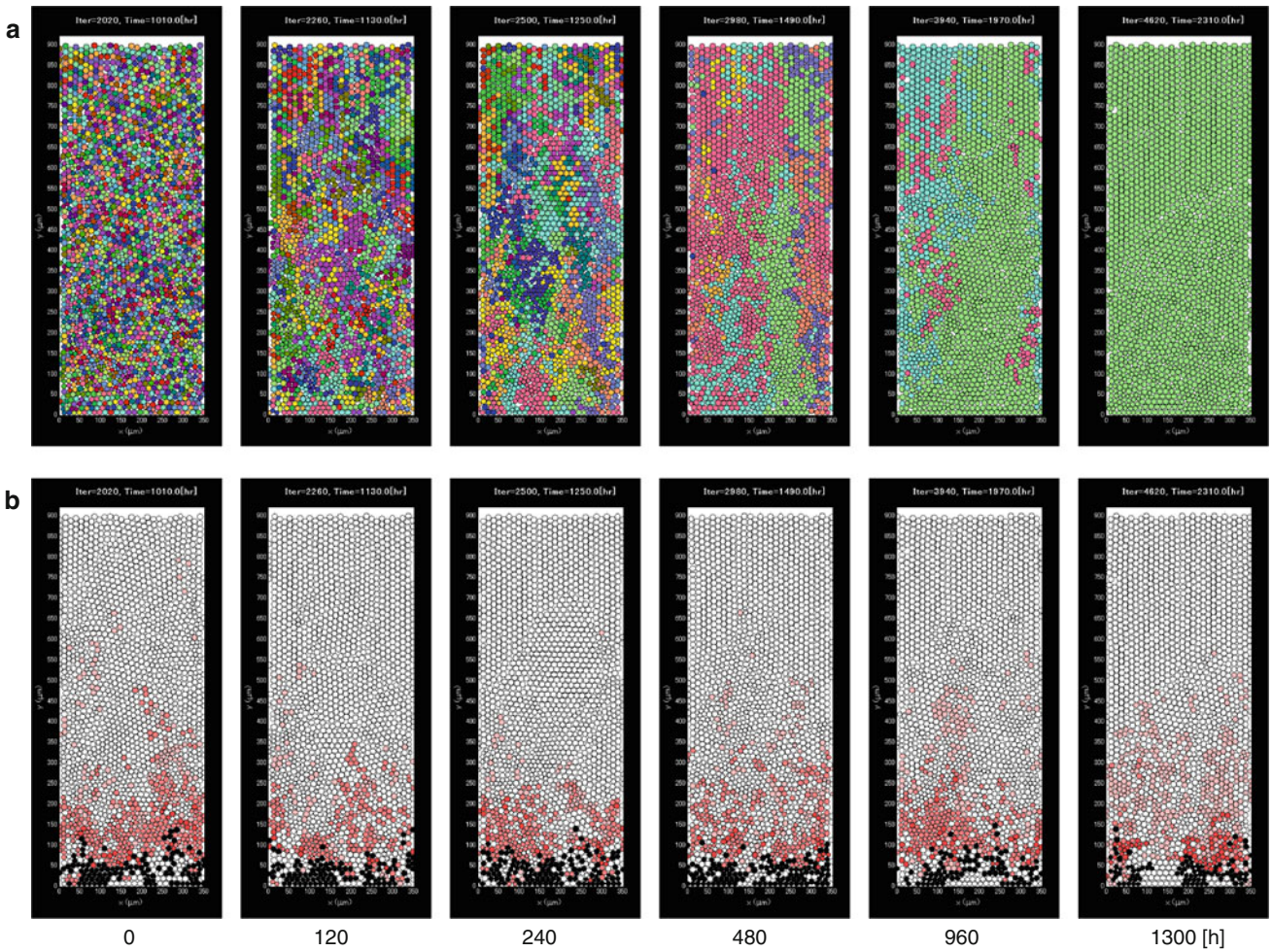

Fig. 2 An example simulation of the monoclonal conversion. **a** Cells at an arbitrary time ($t = 0$ h) are stained with various colors, and expansion of descendants stained with the same color are shown. In this simulation, monoclonal conversions occur, i.e., the crypt is occupied by descendants of a single stem cell at $t = 1{,}300$ h. **b** Cells in each image shown in **a** are stained with colors depending on the cell type; *black* for stem cells, *pink* for TA cells, and *white* for differentiated cells

phenotype, which was different from that of wild-type cells. If the mutant cell propagated throughout the crypt, the set of parameter values was replaced with that of the mutant cell, and thus the mutation accumulated in the crypt. In the following, only mutations in stem cells that were positioned at the bottom of the crypt were considered.

The results are shown in Fig. 3a, b, where the resulting P_{accum} are given. When mutations occurred in the stem cell cycle S, mutant cells with a reduced stem cell cycle showed a significantly higher probability of mutation accumulation than that of neutral mutation (Fig. 3a). However, when mutations occurred in the probability p of symmetric division of stem cells, there was no significant difference in P_{accum} between cells with a modulated p ranging from 0.5 to 1.0 and those of neutral mutation (Fig. 3b). We also found that the propensities to accumulate mutations were dependent on the wild-type parameter values (see the supplementary text C provided in Electronic Supplementary Material).

Discussion

Asymmetric divisions of stem cells

The proposed scenario predicts that symmetric, rather than asymmetric, stem cell division occurs frequently near and at the bottom of the crypt, following the calibrated value of the probability of symmetric division of stem cells ($p = 0.9$; see Fig. 1e). This prediction is in agreement with several previous studies using transgenic mice. For example, Lopez-Garcia et al. [22] revealed that stem cells behave as an equipotent population following a pattern of neutral drift. This observation predicted frequent symmetric cell divisions occurring at the crypt base, which were actually observed by analyzing the sister cell orientation [22]. Snippert et al. [23] also reported that most ($Lgr5^{hi}$) stem cell divisions occur symmetrically.

Besides BrdU labeling, one of the available experimental data obtained from human colons is DNA

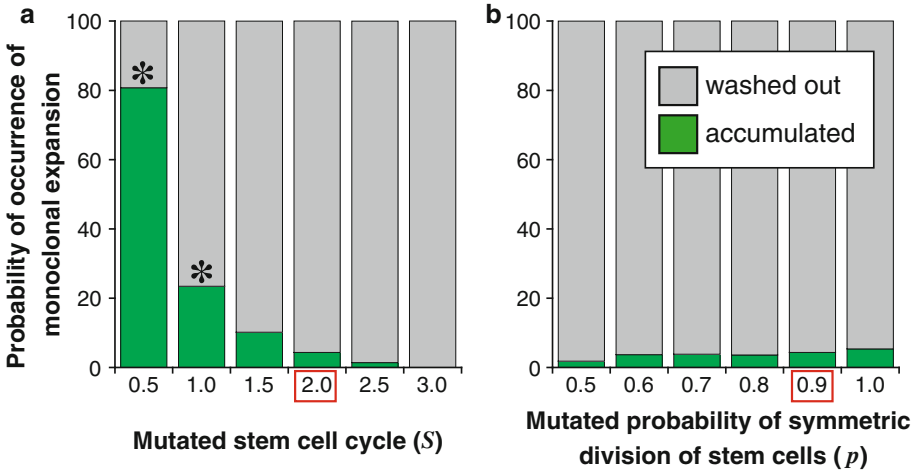

Fig. 3 Results of the simulation of monoclonal expansion of a mutant cell. The probabilities of mutation accumulation in the crypt are shown (*green bars*). These were significantly different from the neutral mutation indicated by *boxed values*. $*P < 0.05$ (Fisher's exact test)

methylation patterns of sampled cells, which have been analyzed to infer aspects of stem cell dynamics by several researchers [4, 5, 24]. According to the recent theoretical work [25], models with purely asymmetric stem cell divisions can mimic colonic stem cell DNA methylation data. This result was different from our prediction that the probability of asymmetric stem cell division was 0.1 ($=1 - p$).

On the other hand, reports on the asymmetric divisions in human colonic crypts are limited at the present time. Although Quyn et al. [26] reported the direct observation of asymmetric division of cells residing at the bottom of the crypt, quantitative data on the frequency of asymmetric divisions of stem cells in human colonic crypts are to be required for critical evaluation of the prediction and for revealing the stem cell dynamics in human colons.

Self-replication region of stem cells

Height of the self-replication region of stem cells, b, can be estimated roughly based on the observation that stem cell marker Lgr5 was present in most cells between positions 1 and 4 in the colonic crypts [26]. Because the mean diameter of the cells is estimated to be $2 \times r_0 \times (1 + \sqrt{2})/2 = 12$ μm in the present model, where $r_0 = 5$ μm is the initial radius of the cell, b can be estimated to be about $4 \times 12 = 48$ μm. Thus, the value of b predicted by the proposed scenario (50 μm; Fig. 1e) was in good agreement with this rough estimation based on the independent experimental data.

Number of stem cells

In the present model, the number of stem cells, defined as able to produce a first-generation TA cell, was introduced explicitly. To meet the labeling index plot given by experiments, the proposed scenario required 100–150 stem cells as a result of the calibrated model parameter values of b and p (see Supplementary Fig. 1b). This number is much larger than that estimated experimentally in a human colonic crypt using putative stem cell markers such as Musashi-1 [27, 28], Lgr5 [29], and aldehyde dehydrogenase 1 [30]. However, the number of stem cells estimated in the model cannot be directly compared with the experimental data, because (1) the stem cells defined in this model were not identical to the cells expressing putative stem cell markers detected in the experiments, and (2) the lower crypt morphology of the model was different from that of a real crypt. As discussed in the following subsection, an excessive number of cells exist near the bottom region, and, therefore, the number of stem cells was overestimated. Development of a three-dimensional crypt model is needed to discuss the number of stem cells more precisely.

Effect of modeling crypts as cylinders

In the present model, crypts were modeled as cylinders. However, the bottom surfaces of real crypts are not open, as in our model, but sealed. To investigate the effect of this geometrical discrepancy, we developed a two-dimensional IB model describing the bottom surface of the crypt (see Supplementary Fig. 8a). Hereafter, we call this model the bottom surface model, whereas the original is called the cylinder model.

In the bottom surface model, we only considered the bottom region of the crypt, which was modeled as a circle with a radius of 87.5 μm, a quarter of the width of the cylinder model (350 μm). Using the same cell model using a parameter set shown in Fig. 1e, where the self-replication region of stem cells was defined as the region within a center circle of a radius $b = 50$ μm, numerical simulations of BrdU labeling experiments were executed. As shown in Supplementary Fig. 8b, there was little difference in the LI

plots between the bottom surface and cylinder models, when the same model parameters were used. On the other hand, as shown in Supplementary Fig. 8c, the mean number of stem cells in a crypt was 50.6 ($n = 3$) in the bottom surface model, which was less than half of that in the cylinder model [128.0 ($n = 3$)]. Therefore, the cylinder model geometry can strongly affect the number of cells residing near the bottom region. In future models, the surface of the model should be reconstructed with the three-dimensional architecture of real colonic crypts.

Limitations of the model

In addition to the issues discussed above, the model has several other limitations. Each of them are presented and discussed below. Understanding these limitations is critical to evaluate the predictions made with the model.

The present model lacked simulation of cell–cell adhesion. To investigate the effect of cell–cell adhesion interactions on the cell dynamics, the BrdU labeling index profiles and the number of stem cells were calculated when the cells attract each other when the distance between their surfaces was less than d_A, by changing the shoving algorithm slightly (see the supplementary text A for the implementation). As a result, up to $d_A = 0.3$ μm, there was no noticeable difference between data obtained with or without cell–cell adhesion interactions (data not shown). Next, we calculated the probability of the accumulation of a neutral mutation introduced in a stem cell positioned at the crypt bottom with an interaction of $d_A = 0.3$ μm. As a result, we found that the probability was about 0.8 % (1/126), which was not significantly different from that obtained without cell–cell adhesion [4.3 % (3/69); the bars indicated by boxed values in Fig. 3a, b] ($p = 0.16$, Fisher's exact test). These results imply that cell–cell adhesion interactions had only a small effect on the cell dynamics discussed in this study. However, we do not exclude the possibility that the cell dynamics change drastically by increasing d_A to more than 0.3 μm in the present model, or by implementing cell–cell adhesion interactions in other modeling frameworks.

If the strength of cell–cell adhesion interactions depends on the cell type, the effect of cell–cell adhesion is thought to significantly impact the cell dynamics. In fact, the axis-aligned phenotype segregation in a crypt can be observed in a model without the signal (e.g. Wnt) gradient along the crypt by introducing a rule in which strong adhesion occurs between the same cell types, while weak adhesion occurs between different cell types [31]. Because the present model corresponded to the model without differential adhesion, proliferative and differentiated cells were intermingled [10, 31]. Also, as modeled by Buske et al. [12] and Dunn et al. [32, 33], interactions between cells and the basal membrane can have a significant effect on the cell dynamics.

Although it would be difficult to introduce contact inhibition into the present model, introducing contact inhibition into a model would have an effect on the cell dynamics in the crypt. In the model developed by Buske et al. [12], the pressure compressing cells is supposed to be high on average when the cell position in a crypt is low, and vice versa, because of the zero pressure condition at the boundary of the upper limit. Thus, cells residing in the lower part of the crypt frequently stop growing because of contact inhibition, and have a longer cell cycle. In fact, by introducing contact inhibition, the wide spectrum of the cell cycle can be described [34]. On the other hand, in the present model, by introducing two proliferative cell types with different mean cell cycle durations, a delay occurred in the cell cycle of cells in the lower part of the crypt.

Another limitation is neglecting apoptosis in the model. The cell number in the model crypt is limited to about 2000 by eliminating cells when they approach the upper limit, rather than considering apoptosis in the crypt. However, apoptosis is essential for homeostasis of the crypt. In the rectosigmoid tract of human subjects with a history of large adenomas, apoptosis is markedly reduced and the balance of cell proliferation and apoptosis is disrupted [35]. Moreover, this imbalance is considered to increase the risk of colon cancer development. Thus, investigating the effect of apoptosis on cell proliferation and differentiation dynamics in the crypt will be important, particularly for investigation of carcinogenesis in the colon.

In addition, to simulate carcinogenesis, it is essential for the model to describe the departure of cells from the epithelial layer. Thus, the model should be expanded by tolerating cells that accumulate in the three-dimensional space.

Conclusion

Through the simulations of the proposed scenario, we have shown the applicability of the computational modeling to verify possible scenarios of stem cell dynamics occurred in human colonic crypts, which are inferred from transgenic mice models. Extending the IB model to a model with three-dimensional architecture of human colonic crypts would allow us to elucidate stem cell dynamics more precisely.

Acknowledgments We thank Takamasa Murano for his assistance with executing the simulation. This study is a part of the outcome of research performed under a Waseda University Grant for Special Research Projects (Project number: 2009B-212). We are also grateful for the helpful suggestions of three reviewers which greatly improved the manuscript.

Conflict of interest The authors declare that they have no conflict of interest.

References

1. Barker N, Ridgway RA, van Es JH, van de Wetering M, Begthel H, van den Born M, et al. Crypt stem cells as the cells-of-origin of intestinal cancer. Nature. 2009;457:608–11.
2. Tian H, Biehs B, Warming S, Leong KG, Rangell L, Klein OD, et al. A reserve stem cell population in small intestine renders Lgr5-positive cells dispensable. Nature. 2011;478:255–9.
3. Taylor RW, Barron MJ, Borthwick GM, Gospel A, Chinnery PF, Samuels DC, et al. Mitochondrial DNA mutations in human colonic crypt stem cells. J Clin Invest. 2003;112:1351–60.
4. Yatabe Y, Tavaré S, Shibata D. Investigating stem cells in human colon by using methylation patterns. Proc Natl Acad Sci USA. 2001;98:10839–44.
5. Nicolas P, Kim KM, Shibata D, Tavaré S. The stem cell population of the human colon crypt: Analysis via methylation patterns. PLoS Comput Biol. 2007;3:0364–74.
6. Graham TA, Humphries A, Sanders T, Rodriguezjusto M, Tadrous PJ, Preston SL, et al. Use of methylation patterns to determine expansion of stem cell clones in human colon tissue. Gastroenterology. 2011;140:1241–50.
7. Fearon ER, Bommer GT. Ancestries hidden in plain sight: methylation patterns for clonal analysis. Gastroenterology. 2011;140:1139–43.
8. Johnston MD, Edwards CM, Bodmer WF, Maini PK, Chapman SJ. Mathematical modeling of cell population dynamics in the colonic crypt and in colorectal cancer. Proc Natl Acad Sci USA. 2007;104:4008–13.
9. Boman BM, Fields JZ, Cavanaugh KL, Guetter A, Runquist OA. How dysregulated colonic crypt dynamics cause stem cell overpopulation and initiate colon cancer. Cancer Res. 2008;68:3304–13.
10. Meineke FA, Potten CS, Loeffler M. Cell migration and organization in the intestinal crypt using a lattice-free model. Cell Prolif. 2001;34:253–66.
11. van Leeuwen IMM, Mirams GR, Walter A, Fletcher A, Murray P, Osborne J, et al. An integrative computational model for intestinal tissue renewal. Cell Prolif. 2009;42:617–36.
12. Buske P, Galle J, Barker N, Aust G, Clevers H, Loeffler M. A comprehensive model of the spatio-temporal stem cell and tissue organisation in the intestinal crypt. PLoS Comput Biol. 2011;7:e1001045.
13. Picioreanu C, Kreft JU, Van Loosdrecht MCM. Particle-based multidimensional multispecies biofilm model. Appl Environ Microbiol. 2004;70:3024–40.
14. Potten CS, Kellett M, Roberts SA, Rew DA, Wilson GD. Measurement of in vivo proliferation in human colorectal mucosa using bromodeoxyuridine. Gut. 1992;33:71–8.
15. Barker N, van Es JH, Kuipers J, Kujala P, van den Born M, Cozijnsen M, et al. Identification of stem cells in small intestine and colon by marker gene Lgr5. Nature. 2007;449:1003–7.
16. Fellous TG, McDonald SAC, Burkert J, Humphries A, Islam S, De-Alwis NMW, et al. A methodological approach to tracing cell lineage in human epithelial tissues. Stem Cells. 2009;27:1410–20.
17. Fearon ER, Vogelstein B. A genetic model for colorectal tumorigenesis. Cell. 1990;61:759–67.
18. Knudson AG. Two genetic hits (more or less) to cancer. Nat Rev Cancer. 2001;1:157–62.
19. Michor F, Iwasa Y, Nowak MA. Dynamics of cancer progression. Nat Rev Cancer. 2004;4:197–205.
20. Wodarz D, Komarova NL. Computational biology of cancer: lecture notes and mathematical modeling. Singapore/Hackensack: World Scientific; 2005.
21. Greaves M, Maley CC. Clonal evolution in cancer. Nature. 2012;481:306–13.
22. Lopez-Garcia C, Klein AM, Simons BD, Winton DJ. Intestinal stem cell replacement follows a pattern of neutral drift. Science. 2010;330:822–5.
23. Snippert HJ, van der Flier LG, Sato T, van Es JH, van den Born M, Kroon-Veenboer C, et al. Intestinal crypt homeostasis results from neutral competition between symmetrically dividing Lgr5 stem cells. Cell. 2010;143:134–44.
24. Walters K. Colonic stem cell data are consistent with the immortal model of stem cell division under non-random strand segregation. Cell Prolif. 2009;42:339–47.
25. Walters K. Parameter estimation for an immortal model of colonic stem cell division using approximate Bayesian computation. J Theoret Biol. 2012;306:104–14.
26. Quyn AJ, Appleton PL, Carey FA, Steele RJC, Barker N, Clevers H, et al. Spindle orientation bias in gut epithelial stem cell compartments is lost in precancerous tissue. Cell Stem Cell. 2010;6:175–81.
27. Nishimura S, Wakabayashi N, Toyoda K, Kashima K, Mitsufuji S. Expression of Musashi-1 in human normal colon crypt cells: a possible stem cell marker of human colon epithelium. Dig Dis Sci. 2003;48:1523–9.
28. Samuel S, Walsh R, Webb J, Robins A, Potten C, Mahida YR. Characterization of putative stem cells in isolated human colonic crypt epithelial cells and their interactions with myofibroblasts. Am J Physiol Cell Physiol. 2009;296:C296–305.
29. Becker L, Huang Q, Mashimo H. Immunostaining of Lgr5, an intestinal stem cell marker, in normal and premalignant human gastrointestinal tissue. Sci World J. 2008;8:1168–76.
30. Huang EH, Hynes MJ, Zhang T, Ginestier C, Dontu G, Appelman H, et al. Aldehyde dehydrogenase 1 is a marker for normal and malignant human colonic stem cells (SC) and tracks SC overpopulation during colon tumorigenesis. Cancer Res. 2009;69:3382–9.
31. Wong SY, Chiam KH, Lim CT, Matsudaira P. Computational model of cell positioning: directed and collective migration in the intestinal crypt epithelium. J R Soc Interface. 2010;7:S351–63.
32. Dunn SJ, Fletcher AG, Chapman SJ, Gavaghan DJ, Osborne JM. Modelling the role of the basement membrane beneath a growing epithelial monolayer. J Theoret Biol. 2012;298:82–91.
33. Dunn SJ, Appleton PL, Nelson SA, Näthke IS, Gavaghan DJ, Osborne JM. A two-dimensional model of the colonic crypt accounting for the role of the basement membrane and pericryptal fibroblast sheath. PLoS Comput Biol. 2012;8:e1002515.
34. Byrne H, Drasdo D. Individual-based and continuum models of growing cell populations: a comparison. J Math Biol. 2009;58:657–87.
35. Anti M, Armuzzi A, Morini S, Iascone E, Pignataro G, Coco C, et al. Severe imbalance of cell proliferation and apoptosis in the left colon and in the rectosigmoid tract in subjects with a history of large adenomas. Gut. 2001;48:238–46.